Supporting Information

4.9% Au stabilizes Ag in atomically homogenous bimetallic alloy for anisotropic nanocrystals with enhanced stability under light irradiation

Zhenying Xu, Hao Xie, Weixiang Ye, Yi Yang, and Weihai Ni*

METHODS

Chemicals. Cetyltrimethylammonium bromide (CTAB), cetyltrimethylammonium chloride (CTAC), silver nitrate ($AgNO_3$), L-ascorbic acid (AA), sodium hypochlorite (NaOCl), and sodium borohydride ($NaBH_4$) were obtained from Sigma-Aldrich. Tetrachloroauric (III) acid ($HAuCl_4 \cdot 3H_2O$) was obtained from Acros. Hydrochloric acid (HCl, 36%), sodium hydroxide (NaOH), hydrogen peroxide (H_2O_2, 30%), nitric acid (HNO_3, 65%), and ammonia water (NH_4OH, 25%) were obtained from Sinopharm Chemical Reagent Co. Deionized (DI) water (18.2 MΩ) was provided by Milli-Q ultrapure water system. All chemicals were used without further purification.

Growth of starting Au NRs. Starting Au NRs were grown using the silver ion-assisted seed-mediated method. Typically, the seed solution was prepared by the addition of $HAuCl_4$ (0.01 M, 0.25 mL) into CTAB (0.1 M, 10 mL) in a 20-mL glass bottle with gentle mixing. A freshly prepared, ice-cold $NaBH_4$ solution (0.01 M, 0.6 mL) was then injected quickly into the mixture solution, followed by rapid inversion for 2 min. The seed solution was kept at room temperature for at least 2 h before use. To grow Au NRs, $HAuCl_4$ (0.01 M, 2.0 mL) and $AgNO_3$ (0.01 M, 0.4 mL) were mixed with CTAB (0.1 M, 40 mL) in a 50-mL plastic tube. HCl (1.0 M, 0.8 mL) was then added to adjust the pH of the solution to 1–2, followed by the addition of ascorbic acid (0.1 M, 0.32 mL). Finally, the seed solution (0.096 mL) was injected into the growth solution. The solution was gently mixed for 10 s and grown overnight at room temperature. The as-synthesized Au NRs are monodispersed and possess an ensemble LSPR wavelength at 834 nm. Their average width, length, and aspect ratio are 18.3 ± 1.9 nm, 72.6 ± 6.0 nm, and 4.0 ± 0.6, respectively.

Overgrowth of AuAg alloys on Au NRs. The starting Au NRs (6 mL) were washed twice by centrifugation and redispersed in 10 mM CTAC (0.6 mL). The growth solution was prepared by mixing 1 mL of 0.1 M CTAC and $AgNO_3$, NH_4OH, and $HAuCl_4$ solutions according to Table S1. The volume of the growth solution was adjusted to 10 mL by adding a calculated volume of DI water. The resultant concentration of CTAC in the growth solution was 10 mM.

0.6 mL of the Au NR solution was then added to the growth solution, followed by gently mixing for 10 sec. To start the overgrowth, a calculated volume of 0.1 M AA was added at a low rate of 40 μL/min with gentle mixing. The solution mixture was kept undisturbed overnight at room temperature.

Oxidation of the Au@AuAg NRs. The Au@AuAg NRs (0.5 mL) were washed by centrifugation and redispersed in CTAC (10 mM, 1 mL). H_2O_2 (0.1 M, 50 μl) was added to the NR solution to start the oxidation.

ICP measurement. 1 mL of the Au@AuAg NR solution was washed by centrifugation and redispersed into 0.9 mL of DI water. 50 μL of 0.1 M HNO_3 and 15 μL of 0.2 M NaOCl were added to the Au@AuAg NR solution, and the solution was mixed by inversion. 50 μL of aqua regia was added after 3 hs. After another 3 hs, 100 μL of NH_4OH (25%) was added, and the solution became clear. It was diluted to 6 mL with DI water. The whole process was performed in dark. ICP measurements were performed on Vista-MPX with axially or radially viewed plasma, free running air-cooled, 40 MHz RF generator, purged echelle polychromator and thinned back-illuminated MegaPixel (MPX) Charge Coupled Device (CCD) detector.

Single-particle stability measurement of Au@AuAg NRs under light irradiation. The Au@AuAg NRs were deposited on a clean glass substrate and rinsed with ethanol to remove the CTAB. A custom spectral imaging dark-field microscope setup was employed to study the stability of individual Au@AuAg NRs. The setup consists of an upright microscope Zeiss Axioscope 5 with an EC-Epiplan 60x/0.75 Zeiss objective, oil-immersion darkfield condenser (NA = 1.2-1.4), a Halogen Lamp (OSL2, Thorlabs), and a liquid crystal tunable bandpass filter (KURIOS-VB1, Thorlabs). The scattered light of the Au@AuAg NRs in the field of view (FOV) was collected by a CMOS camera (Hamamatsu orca flash V4.0). For automated data acquisition and analysis, we used a home-written MATLAB-based software. The plasmon resonance wavelength, linewidth, and maximum intensity of all the particles in the FOV were extracted by fitting the scattering spectrum with a Lorentzian function, allowing for the simultaneous measurement of all the nanoparticles (1000–2000) with relatively high precision and temporal resolution (e.g., 1 min for all spectra). 40 wavelengths were measured for each spectrum with the exposure time of 1 sec for each wavelength. The Au@AuAg NRs were measured every 1 h and in total for 10-24 h. The sample was constantly irradiated by the halogen lamp (HAL 100, Zeiss) at its half intensity except for the time interval of the spectral measurements.

Calculation of Au fraction in the alloy shell.

$$V_{Au} = V_{Core} + V_{Au\_shell} \tag{1}$$

$$V_{Ag} = V_{Ag\_shell} \tag{2}$$

$$V_{Core} = A \times (V_{Ag\_shell} + V_{Au\_shell}) = A \times V_{shell} \tag{3}$$

where A is the volume ratio between the core and shell of the Au@AuAg NR. On the basis of Equation (1-3), one can obtain

$$\frac{V_{Au\_shell}}{V_{Ag}} = \frac{\frac{V_{Au}}{V_{Ag}} - \frac{V_{Core}}{V_{shell}}}{1 + \frac{V_{Core}}{V_{shell}}} \tag{4}$$

The volume fraction of Au in the alloy shell can be finally obtained

$$\frac{V_{Au\_shell}}{V_{shell}} = \frac{V_{Au\_shell}}{V_{Au\_shell} + V_{Ag}} = \frac{\frac{V_{Au\_shell}}{V_{Ag}}}{\frac{V_{Au\_shell}}{V_{Ag}} + 1} = \frac{\frac{V_{Au}}{V_{Ag}} - \frac{V_{Core}}{V_{shell}}}{\frac{V_{Au}}{V_{Ag}} + 1} \tag{5}$$

Table S1. Preparation of the growth solution for various Au^{3+}/Ag^{+} ratios.

$Au^{3+}:Ag^{+}$	10 mM $AgNO_3$ (μl)	1M NH_4OH (μl)	10 mM $HAuCl_4$ (μl)	0.1 M AA (μl)
100:0	0	0	532	85.2
96:4	21.3	3.4	510.7	90.9
93:7	37.2	6	494.8	98.7
90:10	53.2	8.6	478.8	104.5
89:11	58.5	9.4	473.5	106.5
83:17	90.5	14.5	441.6	118.2
80:20	106.4	17.1	425.6	124
70:30	159.6	25.6	372.4	143.4
60:40	212.8	34.1	319.2	162.8
50:50	266	42.6	266	182.2
40:60	319.2	51.1	212.8	201.6
30:70	372.4	59.6	159.6	221.1
20:80	425.6	68.1	106.4	240.5
17:83	441.6	70.7	90.4	246.3
15:85	452.2	72.4	79.8	250.2
10:90	478.8	76.6	53.2	259.9
0:100	532	85.1	0	279.3

Table S2. ICP measured amounts of Ag and Au in the Au@AuAg NR samples.

Au^{3+}:Ag^{+}	Ag (mg/L)	Au (mg/L)	V_{Ag}(10^{-8}cm^3)	V_{Au}(10^{-8}cm^3)
100:0	0.00(0.00)	13.17(0.21)	0.00(0.00)	409.13(6.65)
96:4	0.37(0.08)	13.19(0.21)	20.82(4.59)	409.70(6.66)
93:7	0.52(0.08)	13.34(0.22)	29.39(4.63)	414.36(6.71)
90:10	0.77(0.09)	10.89(0.19)	44.02(4.79)	338.18(5.91)
89:11	0.86(0.09)	11.94(0.20)	48.77(4.84)	370.73(6.25)
83:17	1.07(0.09)	11.55(0.20)	60.97(4.97)	358.79(6.13)
80:20	1.04(0.09)	8.98(0.17)	59.04(4.95)	278.91(5.28)
70:30	1.63(0.09)	6.51(0.14)	92.98(5.32)	202.12(4.48)
60:40	2.00(0.10)	5.89(0.14)	113.74(5.55)	182.94(4.28)
50:50	1.86(0.10)	3.30(0.11)	106.15(5.47)	102.54(3.43)
40:60	1.23(0.09)	1.65(0.09)	70.02(5.07)	51.07(2.89)
30:70	2.55(0.10)	2.68(0.10)	145.49(5.89)	83.16(3.22)
20:80	2.82(0.11)	2.67(0.10)	160.87(6.06)	83.01(3.22)
17:83	2.90(0.11)	2.58(0.10)	165.41(6.11)	80.10(3.19)
15:85	2.71(0.11)	2.90(0.11)	154.24(5.99)	90.15(3.30)
10:90	3.57(0.11)	2.89(0.11)	203.18(6.52)	89.75(3.29)
0:100	3.45(0.11)	2.81(0.11)	196.81(6.45)	87.32(3.27)

Table S3. Statistical measurement on the sizes of the Au@AuAg NRs.[#]

Au^{3+}:Ag^{+}	L_C* (nm)	D_C* (nm)	R_C* (nm)	L_S* (nm)	D_S* (nm)	R_S* (nm)
100:0	NA	NA	NA	86.5(0.4)	29.8(0.2)	2.92(0.26)
96:4	NA	NA	NA	80.5(0.4)	27.2(0.2)	2.98(0.33)
93:7	NA	NA	NA	79.8(0.4)	27.3(0.1)	2.94(0.31)
90:10	NA	NA	NA	84.1(0.5)	30.2(0.2)	2.80(0.28)
89:11	NA	NA	NA	78.1(0.6)	26.1(0.2)	3.01(0.31)
83:17	NA	NA	NA	82.2(0.4)	28.4(0.2)	2.93(0.38)
80:20	70.9(0.6)	17.3(0.2)	4.15(0.65)	87.6(0.6)	27.4(0.2)	3.22(0.43)
70:30	70.3(0.5)	17.2(0.2)	4.16(0.64)	86.9(0.5)	27.3(0.2)	3.20(0.36)
60:40	72.7(0.6)	17.7(0.2)	4.17(0.68)	84.5(0.6)	26.8(0.2)	3.17(0.40)
50:50	71.1(0.8)	17.5(0.2)	4.14(0.73)	84.7(0.8)	29.2(0.3)	2.93(0.40)
40:60	71.0(0.5)	17.1(0.2)	4.24(0.78)	84.3(0.6)	27.2(0.2)	3.14(0.41)
30:70	69.1(0.9)	17.2(0.3)	4.11(0.69)	83.1(0.9)	28.2(0.4)	2.99(0.40)
20:80	71.0(0.6)	17.8(0.2)	4.05(0.59)	86.1(0.6)	29.8(0.3)	2.92(0.34)
17:83	67.2(0.6)	16.9(0.2)	4.04(0.66)	80.0(0.8)	29.3(0.5)	2.78(0.42)
15:85	68.2(0.4)	17.0(0.2)	4.07(0.65)	79.2(0.6)	27.6(0.3)	2.90(0.36)
10:90	69.9(0.7)	17.3(0.2)	4.11(0.65)	83.3(0.9)	30.4(0.4)	2.78(0.34)
0:100	69.2(0.6)	17.3(0.2)	4.08(0.58)	80.0(0.7)	29.4(0.4)	2.78(0.43)

* L_C, D_C, and R_C are the length, width, and aspect ratio of the Au core. L_S, D_S, and R_S are the length, width, and aspect ratio of the Ag shell.
# Standard errors are used for the calculation.

Table S4. Calculation of the Au fraction in the alloy shell.[#]

Au^{3+}:Ag^{+}	V_{Core}(nm^3)	V_{shell}(nm^3)	V_{Au}/V_{Ag}	V_{core}/V_{shell}	V_{Au_shell}/V_{shell}	N_{Au_shell}/N_{shell}
100:0	15674(256)*	37669(647)	∞	0.41 (0.01)	1.000 (0.000)	1.000 (0.000)
96:4	15674(256)*	25648(559)	19.68(4.30)	0.61 (0.02)	0.922 (0.016)	0.923 (0.016)
93:7	15674(256)*	25598(538)	14.10(2.23)	0.61 (0.02)	0.893 (0.016)	0.894 (0.016)
90:10	15674(256)*	37382(712)	7.68(0.85)	0.42 (0.01)	0.837 (0.016)	0.837 (0.016)
89:11	15674(256)*	21406(687)	7.60(0.77)	0.73 (0.03)	0.799 (0.018)	0.800 (0.018)
83:17	15674(256)*	30397(845)	5.89(0.49)	0.52 (0.02)	0.780 (0.016)	0.781 (0.016)
80:20	15343(320)	31043(820)	4.72(0.41)	0.49 (0.02)	0.739 (0.019)	0.740 (0.019)
70:30	14959(303)	30680(706)	2.17(0.13)	0.49 (0.01)	0.531 (0.020)	0.533 (0.020)
60:40	16421(327)	26291(683)	1.61(0.09)	0.62 (0.02)	0.377 (0.021)	0.379 (0.022)
50:50	15634(445)	34673(1291)	0.97(0.06)	0.45 (0.02)	0.262 (0.023)	0.263 (0.025)
40:60	15014(327)	28619(811)	0.73(0.07)	0.52 (0.02)	0.118 (0.035)	0.119 (0.037)
30:70	14751(553)	31128(1434)	0.57(0.03)	0.47 (0.03)	0.062 (0.021)	0.063 (0.027)
20:80	16136(347)	36982(1037)	0.52(0.03)	0.44 (0.02)	0.053 (0.018)	0.053 (0.021)
17:83	13830(373)	33534(1505)	0.48(0.03)	0.41 (0.02)	0.048 (0.018)	0.049 (0.023)
15:85	14232(276)	27599(871)	0.58(0.03)	0.52 (0.02)	0.043 (0.020)	0.044 (0.023)
10:90	15077(401)	37879(1484)	0.44(0.02)	0.40 (0.02)	0.030 (0.015)	0.030 (0.020)
0:100	14898(419)	32586(1155)	0.44(0.02)	0.46 (0.02)	-0.009 (0.017)	-0.009 (0.022)

* V_{core} for Au^{3+}:Ag^{+} in the range from 83:17 to 100:0 takes the value of the starting Au NRs.
# Standard errors are used for the calculation.

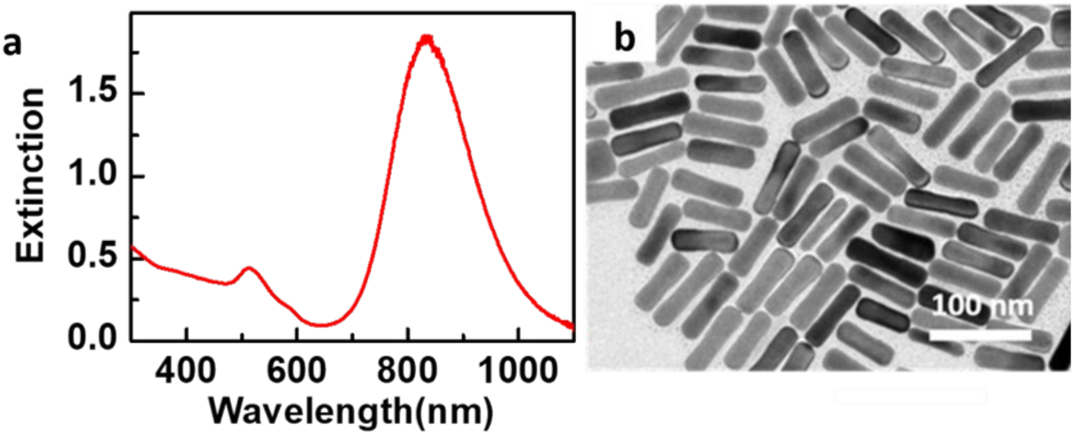

Figure S1. (a) Extinction spectrum of starting Au NRs. (b) Corresponding TEM image.

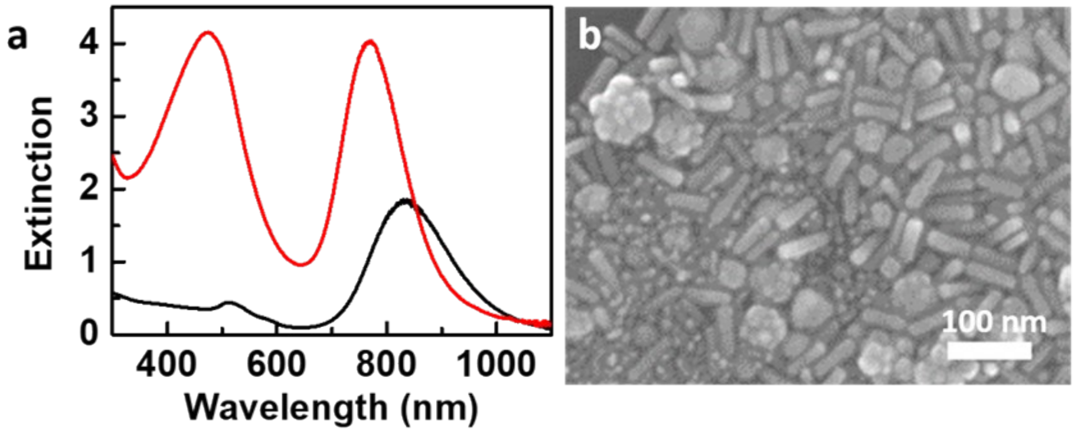

Figure S2. (a) Extinction spectrum of the sample prepared by mixing the starting Au NRs with the growth solution after the addition of AA (red). That of the starting AuNRs is also shown (black). (b) Corresponding SEM image.

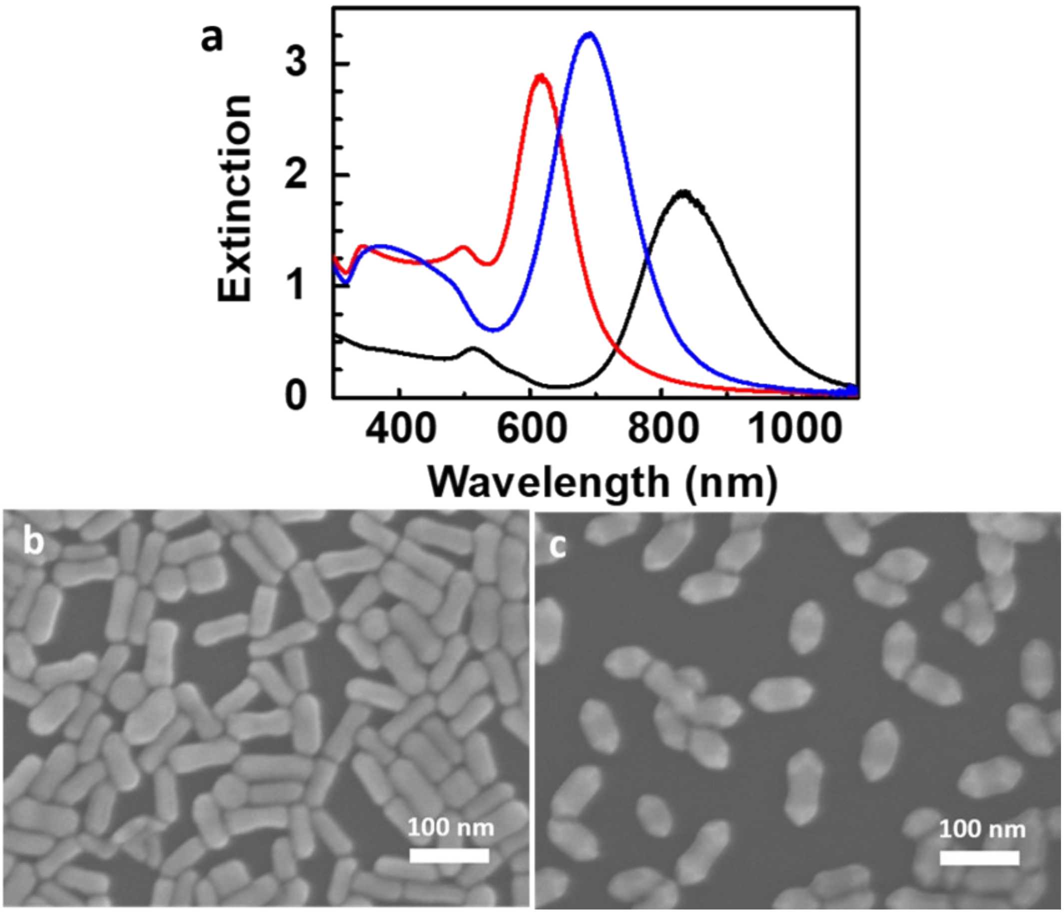

Figure S3. (a) Extinction spectra of the Au@AuAg NR samples prepared with (blue) and without NH_4OH (red). That of the starting Au NRs is also shown (black). (b) SEM image of the Au@AuAg NRs prepared with NH_4OH. (c) That of the Au@AuAg NRs prepared without NH_4OH. The ratio of Ag^+/Au^+ in the growth solution is fixed at 3:2.

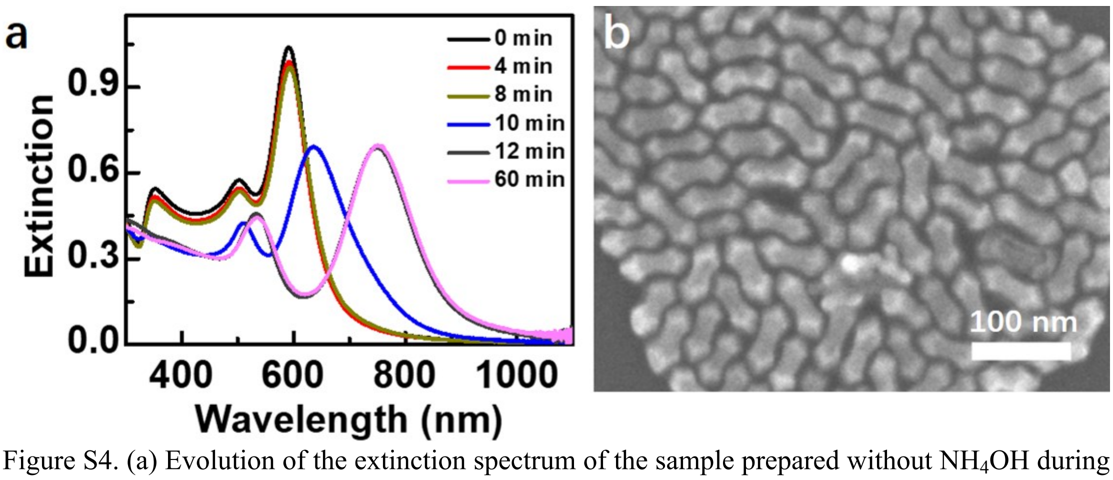

Figure S4. (a) Evolution of the extinction spectrum of the sample prepared without NH_4OH during oxidation. The longitudinal SPR peak is red shifted, indicating the loss of Ag. (b) SEM image of the nanocrystals after the oxidation.

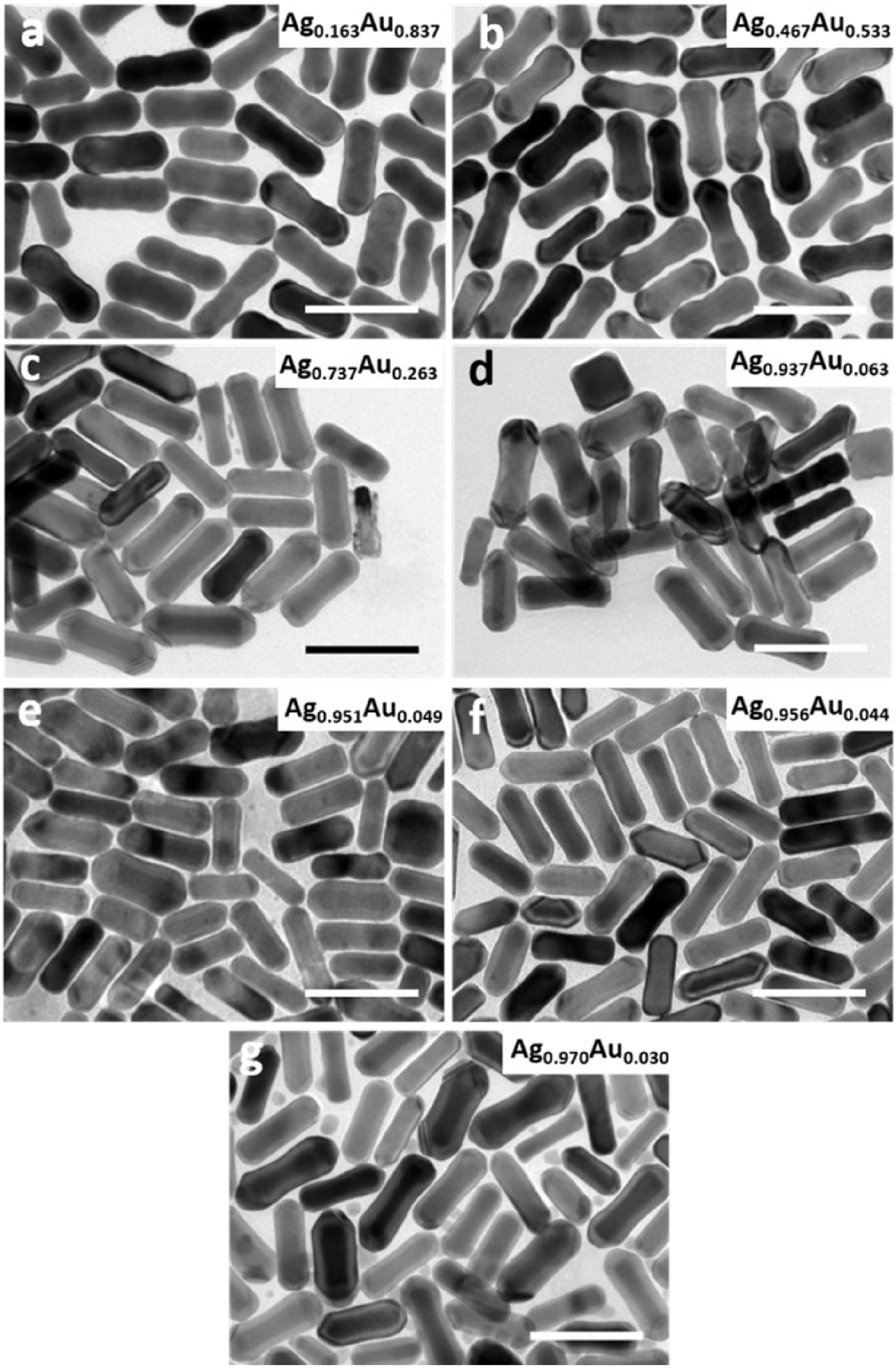

Figure S5. TEM images of Au@AuAg NRs with Ag and Au fractions of the shells labelled. Scale bars 100 nm.

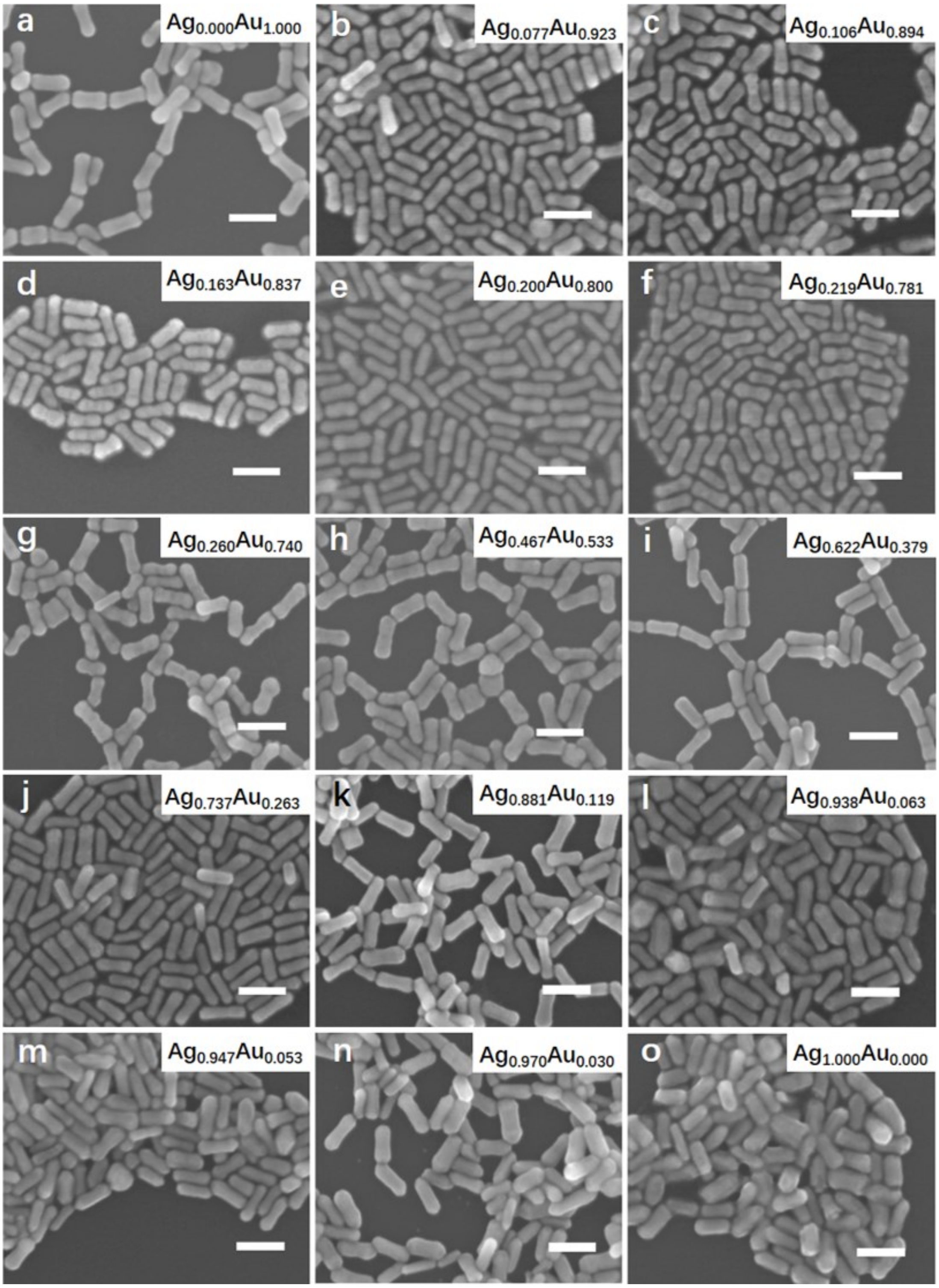

Figure S6. SEM images of Au@AuAg NRs with Ag and Au fractions of the shells labelled. Scale bars 100 nm.

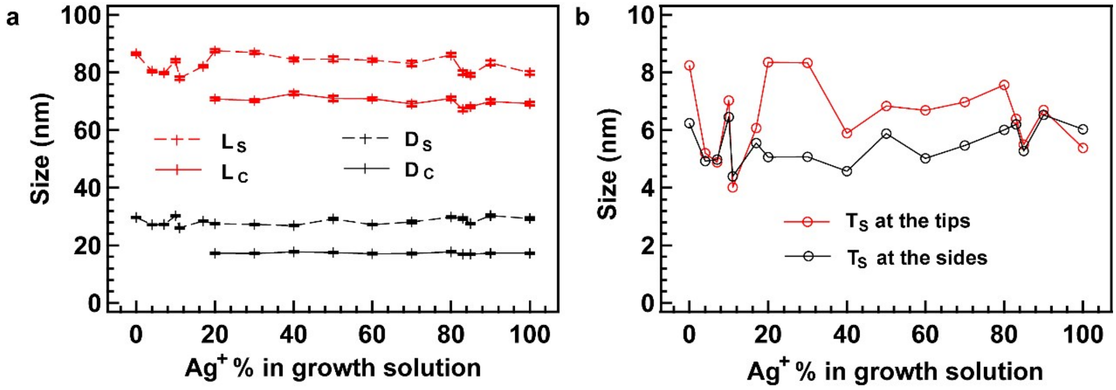

Figure S7. (a) Shell length (L_s), core length (L_c), shell diameter (D_s), and core diameter (D_c) of the Au@AuAg core-shell structures are plotted as a function of Ag^+% in the growth solutions according to the statistical TEM measurements (Table S3). (b) Thickness of the shell (Ts) at the tips and sides are plotted as a function of Ag^+% in the growth solutions.

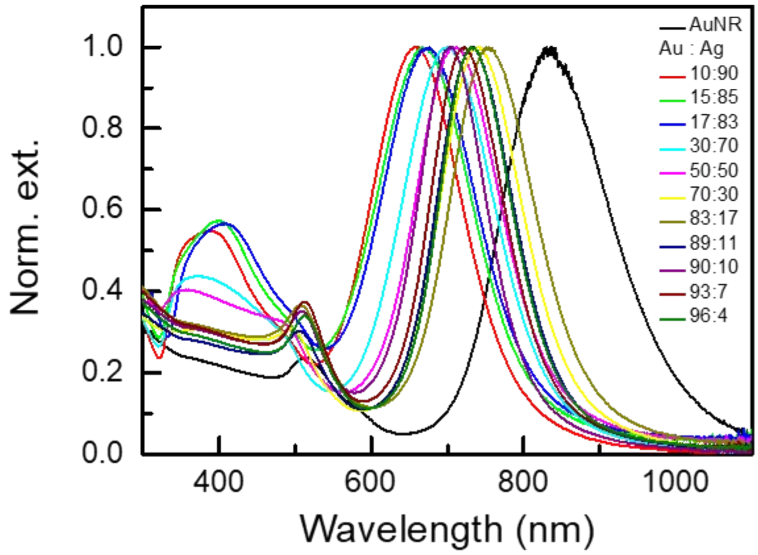

Figure S8. Normalized extinction spectra of Au@AuAg NR solution samples prepared with the growth solutions of various Au/Ag ratio. The starting AuNR sample is also shown (black).

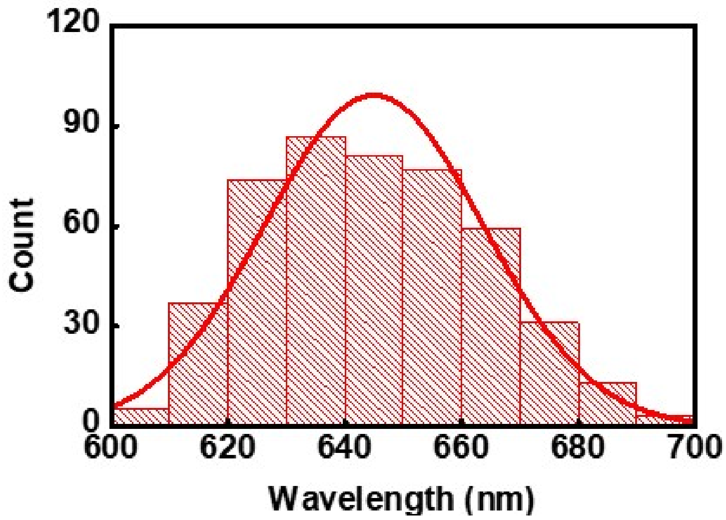

Figure S9. Histograms of the LPR wavelength of the Au@Ag NRs.

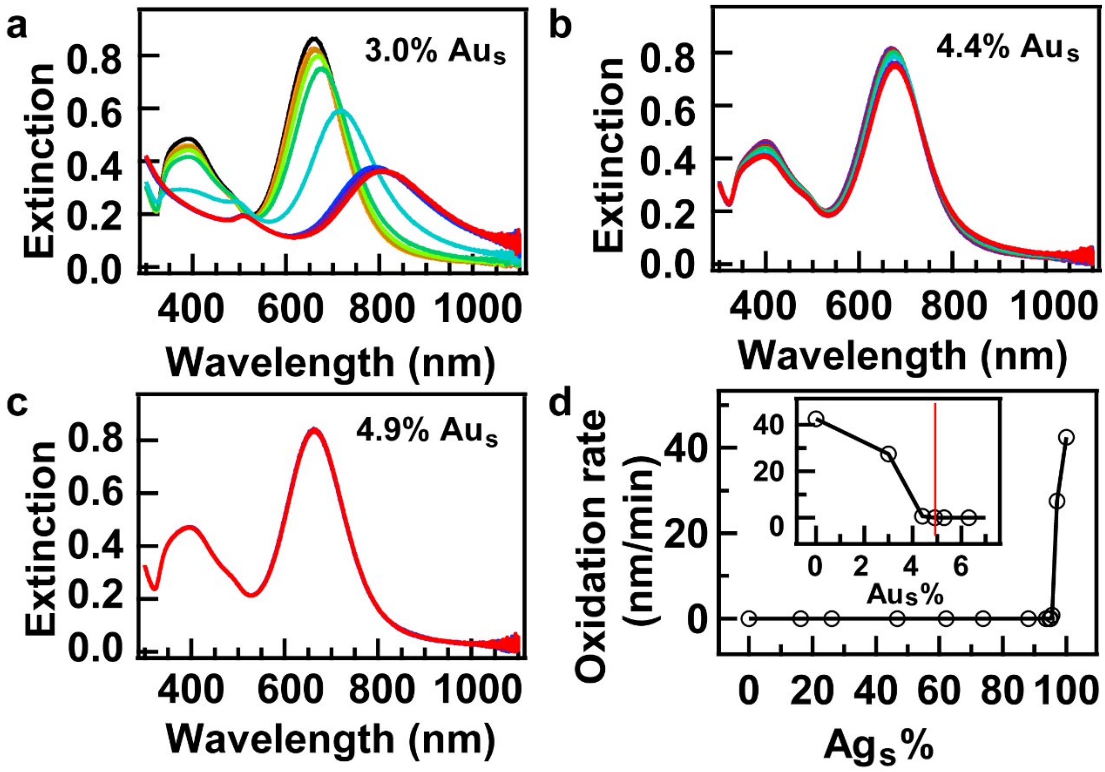

Figure S10. (a-c) Evolution of the extinction spectra of Au@AuAg NRs with Au_s% increasing from 3.0 to 4.4 and 4.9% in the presence of aqueous H_2O_2, respectively. (d) Oxidation rate of the Au@AuAg NRs as a function of Ag_s%. The inset shows the oxidation rate as a function of Au_s%.

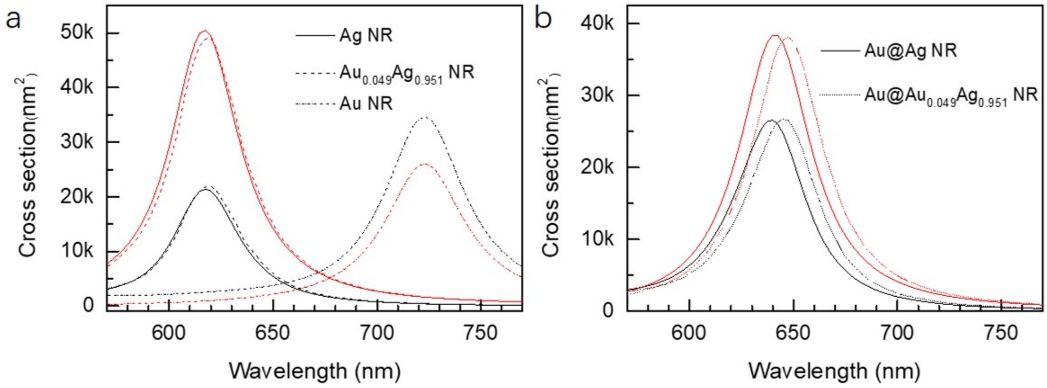

Figure S11. (a) Simulated scattering (red) and absorption (black) spectra of the Ag, $Ag_{0.951}Au_{0.049}$, and Au NRs, respectively. (b) Simulated scattering (red) and absorption (black) spectra of Au@Ag and Au@$Ag_{0.951}Au_{0.049}$ NRs. Bruggeman model is employed for the dielectric function of the AuAg alloy. The width, length, and aspect ratio of the NR are 29.4 nm, 80 nm, and 2.7, respectively.